Sensors and Actuators A 278 (2018) 111–126

Contents lists available at ScienceDirect

Sensors and Actuators A: Physical

journal homepage: www.elsevier.com/locate/sna

Sensitivity of compositional measurement of high-pressure fluid mixtures using microcantilever frequency response

Shadi Khan Baloch[a], Alexandr Jonáš[b], Alper Kiraz[a,d,f], B. Erdem Alaca[e,g], Can Erkey[c,f,*]

[a] Department of Electrical and Electronics Engineering, Koç University, Istanbul, 34450, Turkey
[b] The Czech Academy of Sciences, Institute of Scientific Instruments, Královopolská 147, Brno, 61264, Czech Republic
[c] Department of Chemical and Biological Engineering, Koç University, Istanbul, 34450, Turkey
[d] Department of Physics, Koc University, Istanbul, 34450, Turkey
[e] Department of Mechanical Engineering, Koç University, Istanbul, 34450, Turkey
[f] Koç University Tüpras Energy Center (KUTEM), Koç University, Istanbul, 34450, Turkey
[g] Koç University Surface Technologies Research Center (KUYTAM), Koç University, Istanbul 34450, Turkey

ARTICLE INFO

Article history:
Received 14 February 2018
Received in revised form 26 April 2018
Accepted 14 May 2018
Available online 17 May 2018

Keywords:
Microcantilever
Sensitivity
High pressure
Ethanol
Carbon dioxide
Frequency response

ABSTRACT

Frequency response of an oscillating microcantilever immersed in a fluid mixture can be used to determine the composition of the mixture over a wide range of temperatures and pressures. The Limit of Detection (LOD) in such measurements carried out at high pressures is of great interest for monitoring technologically important processes such as supercritical drying of aerogels. We studied compositional measurement sensitivity of cantilevers defined as the derivative of the cantilever resonant frequency or quality factor with respect to the fluid mixture composition. On the basis of Sader's model of hydrodynamic interaction of an oscillating immersed cantilever with the surrounding fluid, we derived analytical expressions for the sensitivity that were found to be complex functions of the density and viscosity of the mixture as well as the length, width, thickness, and density of the cantilever. We measured the frequency response of cantilevers immersed in ethanol–CO_2 mixtures containing 0 – 0.04 wt fraction of ethanol at 318 K and within the pressure range 10–21 MPa. Using the measured resonant frequency and quality factor together with previously published density and viscosity data for ethanol–CO_2 mixtures of various compositions, we calculated the sensitivity at each pressure and temperature and determined the LOD of the measurement. In particular, with our current setup, the LOD ranged from 0.0009 to 0.0071 wt fraction of ethanol in the mixture in the pressure range 10–21 MPa for a 150 μm long cantilever. Our results convincingly illustrate the potential of miniature cantilever-based probes for fast and sensitive *in-situ* detection of the composition of fluid mixtures in practical technological processes carried out at high pressures.

1. Introduction

Compact sensors based on cantilevers fabricated from different solid materials have received steadily growing attention for the characterization of pure fluids and fluid mixtures [1–14]. When an oscillating cantilever is immersed in a fluid, the fluid surrounding the cantilever is set in motion. This moving fluid then applies hydrodynamic forces on the cantilever, resulting in a decrease in the resonant frequency and the quality factor (Q-factor) of the cantilever oscillations compared to their values in vacuum [3,15–17]. The change in the resonant frequency and the Q-factor can be subsequently used to measure various thermophysical properties of the fluid such as its density and viscosity [1,2,9,13,18–20] and also to determine the composition of a fluid mixture [4,5,7,14,21–23].

For practical applications of detection techniques that exploit oscillating microcantilevers, it is of utmost importance to quantify their sensitivity and Limit of Detection (LOD), as these parameters directly determine the domain of usability of microcantilever-based analytical devices. There have been a limited number of experimental and theoretical studies in the literature on the sensitivity of microcantilever-based detection systems. For example, Zhao et al. [24] studied the effect of the geometry of a microcantilever on the sensitivity of density

* Corresponding author at: Koç University Tüpras Energy Center (KUTEM), Koç University, Istanbul, 34450, Turkey.
E-mail address: cerkey@ku.edu.tr (C. Erkey).

https://doi.org/10.1016/j.sna.2018.05.025
0924-4247/

measurements and formulated an analytical expression for the sensitivity defined as the derivative of the cantilever resonant frequency with respect to the density of the fluid. They showed that the sensitivity could be improved by decreasing the length and the width of the microcantilever and also by using a higher-order resonant mode. They measured the resonant frequency of microcantilevers immersed in n-pentane, n-hexane, n-heptane, n-octane, and cyclohexane with densities ranging from 621 to 774 kg/m^3 and calculated the best resolution of their density measurements as 0.057 kg/m^3 for a 1.9 mm long rectangular cantilever. Boudjiet et al. [7] also showed that the sensitivity of fluid-density sensors based on uncoated microcantilevers can be improved by optimizing the device geometry. They fabricated microcantilevers of different shapes (in particular, rectangular, U-shaped and T-shaped) and dimensions and measured the concentration of H_2 in mixtures of H_2 and N_2 using cantilever resonant frequencies. They found that shorter and wider rectangular cantilevers exhibited better sensitivity to density changes and cantilever thickness did not affect the sensitivity. For 1% H_2 in the mixture, the relative difference between the model and the measured resonant frequency was 0.3 to 25% for the studied cantilevers. Tetin et al. [5] studied the shift in the resonant frequency of uncoated microcantilevers due to the changes in the density and viscosity of the surrounding fluid. They measured the relative shift in the resonant frequency of an immersed microcantilever due to the addition of CO_2 or He to N_2 and compared the experimentally obtained value of the shift with a theoretical model. They neglected the relatively small effect of viscosity on the observed shift of the resonant frequency and reported the sensitivity and LOD of their microcantilever system. Cox et al. [25] studied laterally vibrating microcantilevers immersed in water and aqueous glycerol solutions and measured the resonant frequency, the Q-factor, and the mass sensitivity of the resonant frequency. The mass sensitivities and the Q-factors of microcantilevers excited laterally were found to be higher than those of transversely excited microcantilevers, thus rendering laterally vibrating microcantilevers more suitable for operation in high-viscosity media. Beardslee et al. [26] studied the resonant frequency and the Q-factor of a cantilever immersed in water. They demonstrated that using the in-plane flexural mode reduces damping and mass loading due to the surrounding fluid and showed that shorter, wider, and thinner cantilevers operated with in-plane flexural modes give the best sensing characteristics. Furthermore, Loui et al. [27], Narducci et al. [28], Beardslee et al. [26] and Hocheng et al.[29] also suggested to optimize the cantilever geometry in order to increase the sensitivity of density measurements. All of the above-discussed experimental and computational studies of sensitivity of cantilever-based detection systems were carried out at a low pressure of the fluid surrounding the cantilever (typically at the atmospheric pressure). In addition, in analyzing measurement sensitivity, these studies largely neglected the effects of the changing fluid viscosity and they did not attempt to use the measured thermophysical properties of the fluid to determine fluid's composition.

In this article, we present a systematic study of the sensitivity of measurement of binary fluid mixtures' composition based on the measurement of frequency response of a microcantilever immersed in the fluid. To this end, we use a model system of ethanol–CO_2 mixtures containing 0 – 0.04 wt fraction of ethanol at a pressure range between 10 MPa and 21 MPa and at 318 K. Such mixtures are frequently encountered in many technological processes such as supercritical drying of aerogels or fabrication of Micro-Electro-Mechanical Systems [30–33]. We define the sensitivities S_f, S_Q of the compositional measurement as the derivatives of the cantilever resonant frequency f_{fluid} or the Q-factor Q with respect to the weight fraction of ethanol in the mixture, w $\left(S_f = \mathrm{d}f_{fluid}/\mathrm{d}w,\ S_Q = \mathrm{d}Q/\mathrm{d}w\right)$, and derive analytical expressions for the sensitivity from Sader's model [16] that includes the effects of viscous forces. Using the model sensitivity and the standard deviations of the resonant frequency and the Q-factor measured at given constant experimental conditions, we estimate LOD of ethanol in ethanol–CO_2 mixtures. To the best of our knowledge, this work represents the first systematic study on the change in the resonant frequency or the Q-factor of immersed cantilevers with the mixture composition that also includes the effect of viscous forces in the sensitivity analysis.

2. Materials and methods

2.1. Materials

CO_2 used in the experiments was supplied by Aligaz Messer with a purity of 99.9%. Ethanol was supplied by Sigma-Aldrich with a purity of 99.8%. Both CO_2 and ethanol were used as received.

2.2. Experimental procedure

Ferromagnetic cantilevers of different lengths made of nickel were produced using standard fabrication methods. The design and fabrication process of the cantilevers were explained in detail in our previous study [3]. The cantilevers used in the present study had nominal lengths of 150 μm and 200 μm, a nominal width of 20 μm, and a thickness of about 1 μm.

The experimental setup, which was described in detail in our previous studies [1,3], consisted of a high-pressure fluid vessel with sapphire windows, a laser, a quadrant photodiode, a CCD camera, lenses, and additional electronic equipment used for the readout of the cantilever frequency response. A schematic diagram of the experimental set-up is given in Fig. 1(a). Before the measurements, a die with cantilevers was mounted in a Teflon housing containing an electromagnetic actuator - a coil made from copper wire - and the housing was subsequently placed in a 50-mL cylindrical high-pressure vessel with two sapphire windows on each side (TharSFC 05424-4). These windows allowed the monitoring of microcantilevers during the experiment and the measurement of their frequency response using laser beam deflection. Electrical connection to the copper coil in the high-pressure vessel was sealed using insulated CONAX Technologies TG24 T-gland assemblies. Temperature of the fluid mixture in the high-pressure vessel was controlled by circulating water through plastic tubing wrapped around the vessel, using a heating circulator with temperature control (LabO C200-H13). The temperature and the pressure in the vessel were continuously monitored using a T-type thermocouple (TC) (Omega dp462) (accuracy ± 1 K) and a pressure transducer (PT) (Omega PX 409-5.0KAUSBH) (accuracy ±0.03 MPa), respectively.

Ethanol–CO_2 mixtures were prepared by successive transfer of ethanol and CO_2 to the high-pressure vessel. The amount of each fluid transferred to the vessel was determined gravimetrically. First, the mass of the empty vessel was measured using a balance with an accuracy of ± 0.1 g. Then, a certain amount of liquid ethanol was placed into the vessel using a micropipette. The amount of added ethanol was determined before the transfer into the vessel with a different balance with an accuracy of ± 0.001 g. Subsequently, CO_2 was transferred

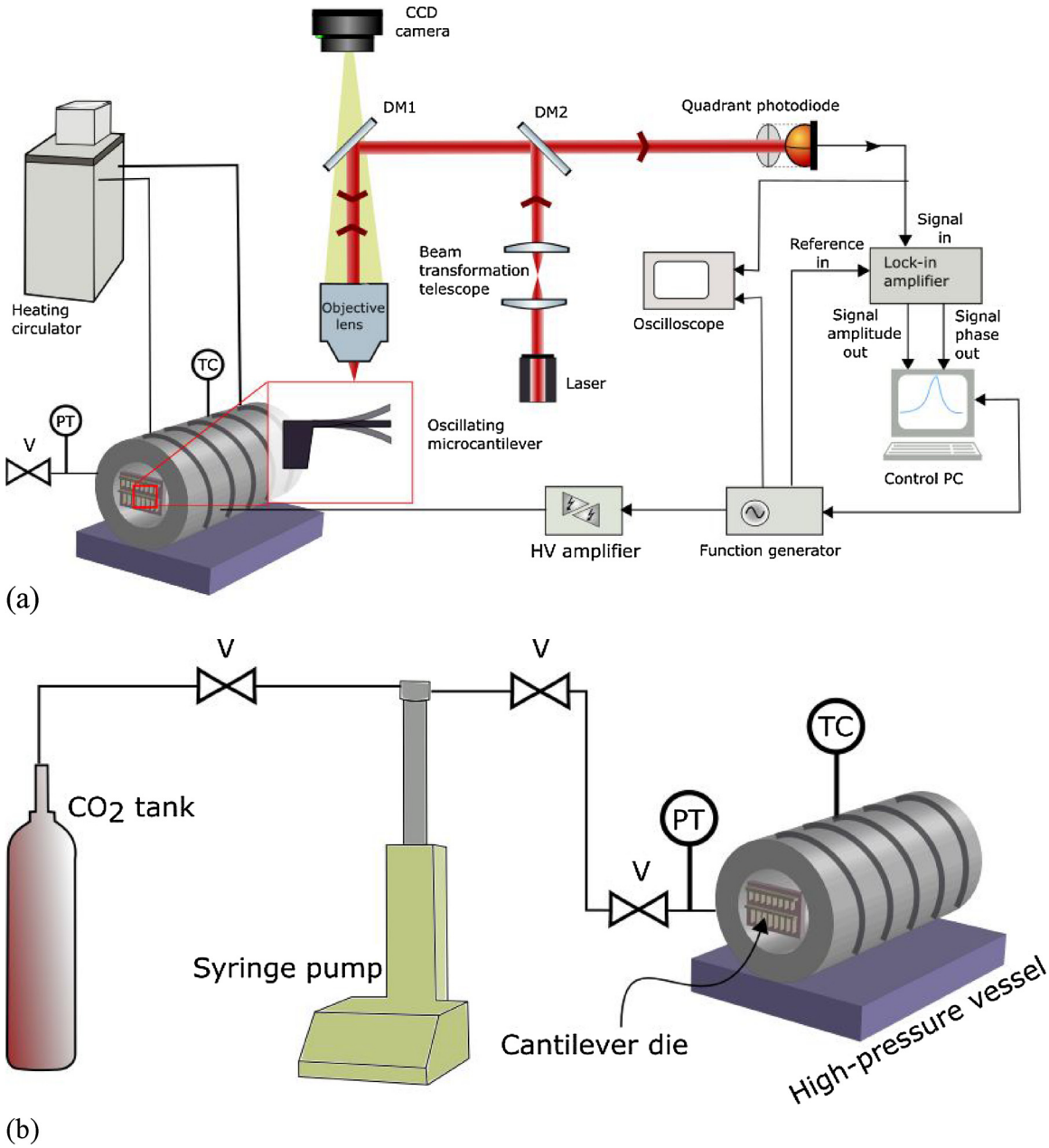

Fig. 1. (a). Schematic drawing of the experimental setup used for measuring the frequency response of immersed microcantilevers. DM1, DM2–dichroic mirrors. (b) Schematic drawing of the system used for sample-chamber pressurization. PT: pressure transducer, TC: thermocouple, V: valve.

Table 1
Measured values of fluid mass and calculated mixture compositions together with uncertainties in individual mass measurements and mixture compositions.

Measured value	Experiment #1	Experiment #2	Experiment #3	Experiment #4	Experiment #5
Empty vessel mass (g)	2185.6 ± 0.1	2185.6 ± 0.1	2185.6 ± 0.1	2185.6 ± 0.1	2185.6 ± 0.1
Ethanol mass (g)	0.791 ± 0.001	1.175 ± 0.001	1.556 ± 0.001	0.335 ± 0.001	0.509 ± 0.001
CO_2 mass (g)	38.4 ± 0.1	38.0 ± 0.1	37.5 ± 0.1	38.7 ± 0.1	38.5 ± 0.1
Total mass (g)	2224.8 ± 0.1	2224.8 ± 0.1	2224.7 ± 0.1	2224.7 ± 0.1	2224.7 ± 0.1
Ethanol weight fraction w	0.02017 ± 0.00007	0.02997 ± 0.00011	0.03979 ± 0.00014	0.00856 ± 0.00003	0.01301 ± 0.00005

to the vessel using a TELEDYNE ISCO D Series syringe pump (see Fig. 1(b) for illustration) and the mass of the vessel with both fluids was again measured using the balance with an accuracy of ± 0.1 g. Finally, the masses of the empty vessel and ethanol were subtracted from the total mass of the filled vessel to determine the amount of CO_2 placed into the vessel. Measured fluid masses and calculated mixture compositions specified in terms of the weight fraction of ethanol in the mixture, w, together with their respective uncertainties, are given in Table 1.

During the measurements, the cantilevers were actuated with a time-varying magnetic field produced by the coil driven by a sinusoidal voltage that was generated by a function generator (Agilent 33220 A) and subsequently amplified by a factor of 50 using a high-voltage amplifier (Falco Systems WMA-300; see Fig. 1(a) for illustration). The frequency and amplitude of the driving sinusoidal signal were computer-controlled using Instrument Control Toolbox in Matlab. The deflections of the vibrating cantilever were detected by an atomic force microscopy-like scheme. A near-infrared laser beam (wavelength 780 nm, maximal power 4.5 mW; CPS 192, Thorlabs) was transformed with a 1:1 telescope consisting of two identical lenses (f = 30 mm) and then focused on the cantilever surface with an objective. The telescope enabled changing the axial position of the laser beam focus with respect to the cantilever surface and, thus, optimizing the cantilever deflection signal for different studied fluids. The beam reflected from the oscillating cantilever was collected by the same objective lens and then focused on a quadrant photodiode (QPD). QPD is sensitive to the position of the beam spot within its surface and can be used to record the changes of the propagation direction of the reflected beam due to cantilever deflection. In order to improve the signal-to-noise ratio, the deflection signal was sent to a lock-in-amplifier (SR530, Stanford Research Systems) together with the reference signal from the function generator. The output of the lock-in amplifier represented by the amplitude of the deflection signal and its phase shift with respect to the driving signal was digitized with a data acquisition card (USB-6008, National Instruments) controlled using Matlab programming environment.

In the beginning of each set of measurements with a given fixed mixture composition, the vessel was filled with the desired amount of ethanol and then charged with CO_2 to a pressure ranging between 21 MPa and 22 MPa. The temperature of the vessel was then adjusted to the desired value using the heating circulator. Frequency response measurements were performed when the pressure and temperature became stable, typically 3–5 hours after starting the heating circulator. The measurements of the cantilever frequency response were performed starting from the highest pressure and then gradually decreasing the pressure for the successive measurements in the set. For all measurements reported in this article, the temperature of the vessel was kept at 318 K and after each pressure change, we waited for approximately 5 min before starting the next measurement to ensure thermal equilibrium was restored in the vessel. At each pressure, the driving frequency of the function generator was adjusted over a range of 16 kHz for 150 μm long cantilever and 12 kHz for 200 μm long cantilever, with the central frequency of the studied spectral band equal to the cantilever resonant frequency. The amplitude of the driving sinusoidal signal before 50-times amplification was set to 2 V peak-to-peak and the cantilever response was then recorded at 400 equidistant points within the above described spectral band. Subsequently, the dissipation-free cantilever resonant frequency, f_{fluid}, and the Q-factor, Q, were determined by fitting the measured frequency response $A(\omega)$ to the equation describing the oscillating elastic cantilever beam as a simple damped harmonic oscillator [16]:

$$A(\omega) = \frac{A_0 4\pi^2 f_{fluid}^2}{\sqrt{\left(\omega^2 - 4\pi^2 f_{fluid}^2\right)^2 + \frac{\omega^2 4\pi^2 f_{fluid}^2}{Q^2}}} \tag{1}$$

where A_0 is the zero-frequency amplitude of the response and $\omega = 2\pi f$ is the angular driving frequency. At each pressure, three consecutive measurements of the cantilever frequency response were carried out and the averages of the three resonant frequencies and Q-factors were reported. For the measurements on 150-μm-long cantilevers, the average relative standard deviations of the resonant frequency and the Q-factor over the whole studied pressure range were 0.04% and 1.12%, respectively, while the maximum relative standard deviations were 0.32% and 3.94%, respectively. For the 200-μm-long cantilever, the average relative standard deviations of the resonant frequency and the Q-factor were 0.05% and 0.89%, respectively, and the maximum relative standard deviations were 0.21% and 3.14%, respectively.

3. Results and discussions

As stated in the introduction, sensitivity S_f of the cantilever resonant frequency f_{fluid} to changes in the weight fraction of ethanol in the mixture w can be defined as the derivative of f_{fluid} with respect to w. Similarly, sensitivity S_Q of the cantilever Q-factor Q to changes in w is given by the derivative of Q with respect to w. Below, we derive analytical expressions for S_f and S_Q on the basis of Sader's model of hydrodynamic interactions [16]. The starting equations of Sader's model for f_{fluid} and Q in Maali's analytical approximation [34] are given by:

$$f_{fluid} = f_{vac}\left[1 + \frac{\pi\rho b}{4\rho_c t}\left(1.0553 + \frac{3.7997}{\sqrt{2\mathrm{Re}}}\right)\right]^{-1/2} \tag{2}$$

$$Q = \frac{\frac{4\rho_c t}{\pi\rho b} + \left(1.0553 + \frac{3.7997}{\sqrt{2\mathrm{Re}}}\right)}{\frac{3.8018}{\sqrt{2\mathrm{Re}}} + \frac{2.7364}{2\mathrm{Re}}} \tag{3}$$

where f_{vac} is the resonant frequency of the cantilever in vacuum, b is the cantilever width, ρ_c is the cantilever density, t is the cantilever thickness, ρ is the mixture density, μ is the mixture viscosity and Re is the Reynolds number $\left(\mathrm{Re} = \frac{2\pi f_{fluid}\rho b^2}{4\mu}\right)$. Eq. (2) represents the definition of f_{fluid} as an implicit function of the fluid parameters ρ, μ that themselves depend on the mixture composition w. The derivative of f_{fluid} with respect to w can be obtained using the implicit function theorem and applying the chain rule (see the details of the derivation in Appendix A) as:

$$S_f^m = \left(\frac{df_{fluid}}{dw}\right)_m = \frac{1}{\left(\left(\frac{f_{vac}}{f_{fluid}}\right)^3 - \frac{3.7997\pi\rho b f_{vac}}{16 f_{fluid}\rho_c t\sqrt{2\mathrm{Re}}}\right)} \times \left\{-\left(\frac{1.0553\pi b f_{vac}}{8\rho_c t} + \frac{3.7997\pi b f_{vac}}{16\rho_c t\sqrt{2\mathrm{Re}}}\right)\frac{\partial\rho}{\partial w} - \left(\frac{3.7997\pi b\rho f_{vac}}{16\rho_c t\mu\sqrt{2\mathrm{Re}}}\right)\frac{\partial\mu}{\partial w}\right\} \tag{4}$$

where the subscript and superscript m stand for "model".

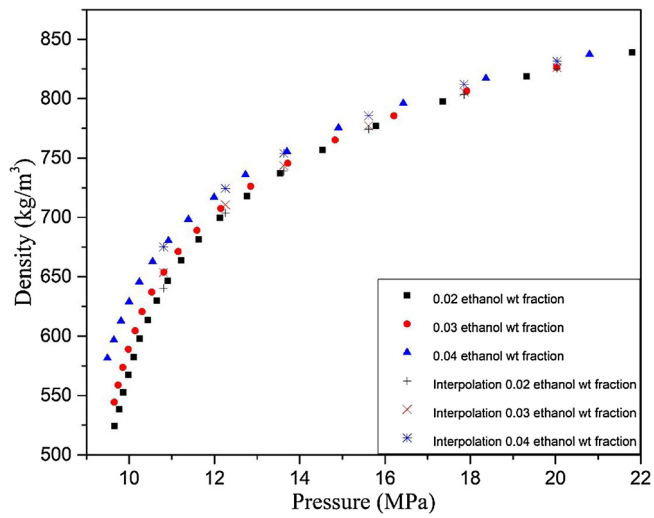

Fig. 2. Change of fluid density with pressure for ethanol–CO_2 mixtures with various compositions at 318 K. Data adopted from Tilly et al. [35], additional data points were determined by cubic-spline interpolation (see text for details).

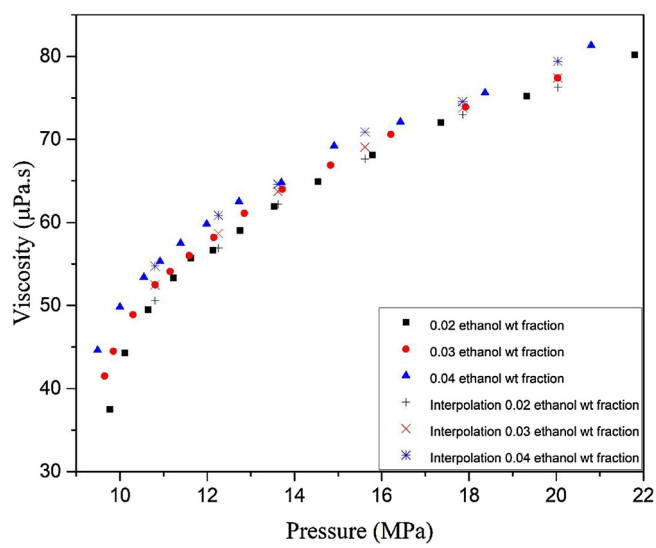

Fig. 3. Change of fluid viscosity with pressure for ethanol–CO_2 mixtures with various compositions at 318 K. Data adopted from Tilly et al. [35], additional data points were determined by cubic-spline interpolation (see text for details).

Eq. (4) is the model - or theoretical - expression for the sensitivity S_f^m ; it shows that S_f^m is a complex function of the density and viscosity of the mixture, as well as cantilever length, width, thickness and cantilever density. In order to evaluate S_f^m for a given experimental condition (pressure, temperature, and composition of the mixture), partial derivatives $\frac{\partial\rho}{\partial w}$ and $\frac{\partial\mu}{\partial w}$ must be determined from the dependence of density and viscosity on the mixture's composition. There are no accurate methods and correlations for estimation of the density and viscosity of fluid mixtures at high pressures. Moreover, there are only very limited experimental data available for the density and viscosity of ethanol–CO_2 mixtures at high pressures in the literature. Viscosity and density of such mixtures containing 2, 3, and 4 mol % of ethanol were measured and reported by Tilly et al. at 318 K and 328 K and a pressure range from 9.48 MPa to 21.8 MPa [35]. We used the data of Tilly et al. [35] recorded at 318 K and applied cubic-spline interpolation to obtain additional values of mixtures' density and viscosity for our particular conditions. Figs. 2 and 3 show how the density and viscosity change with pressure. In order to determine the values of compositional derivatives $\left(\frac{\partial\rho}{\partial w}\right)$ and $\left(\frac{\partial\mu}{\partial w}\right)$ at 318 K and a particular pressure, we used the data in Figs. 2 and 3 together with the data for pure CO_2 ($w = 0$) obtained from the NIST database [36]. The density and viscosity of the fluid were plotted as functions of the ethanol weight fraction w, as shown in Figs. 4 and 5, respectively. Subsequently, for each individual studied pressure, we fitted ρ and μ linearly with w and calculated the compositional derivatives $\left(\frac{\partial\rho}{\partial w}\right)$ and $\left(\frac{\partial\mu}{\partial w}\right)$ from the slopes of the fitted lines at each studied pressure. The values of $\left(\frac{\partial\rho}{\partial w}\right)$ and $\left(\frac{\partial\mu}{\partial w}\right)$ obtained at different pressures are presented in Table 2. As shown in Fig. 5, at a constant pressure and temperature, the viscosity of ethanol–CO_2 mixtures increases with increasing ethanol weight fraction in the mixture. This is a direct consequence of pure ethanol having a higher viscosity than pure CO_2 at the given experimental conditions. It also follows from Fig. 5 that at a constant ethanol weight fraction, w, the viscosity of the mixture increases with pressure. This increase in viscosity is primarily related to the increase of density of ethanol–CO_2 mixtures with increasing pressure (see Fig. 2). At higher densities,

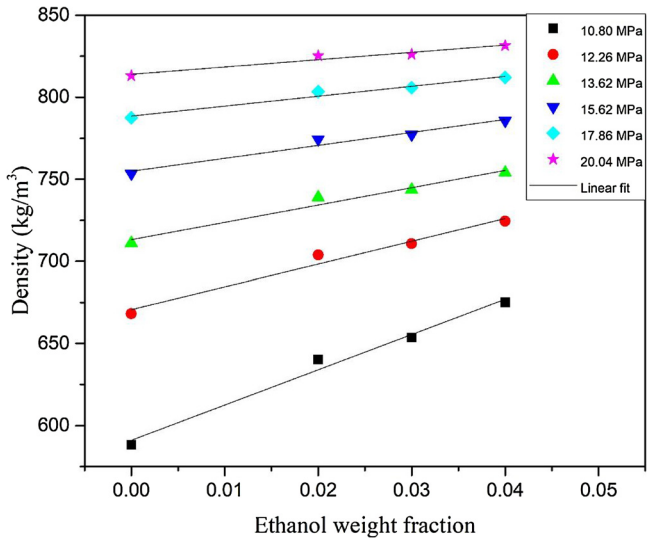

Fig. 4. The dependence of the fluid density, $\boldsymbol{\rho}$, on the ethanol weight fraction, $\boldsymbol{w}$, at different pressures and a fixed temperature of 318 K. Symbols: data points from Tilly et al.[35] ($\boldsymbol{w} \neq 0$)/NIST ($\boldsymbol{w} = 0$), solid lines: linear fits to the data.

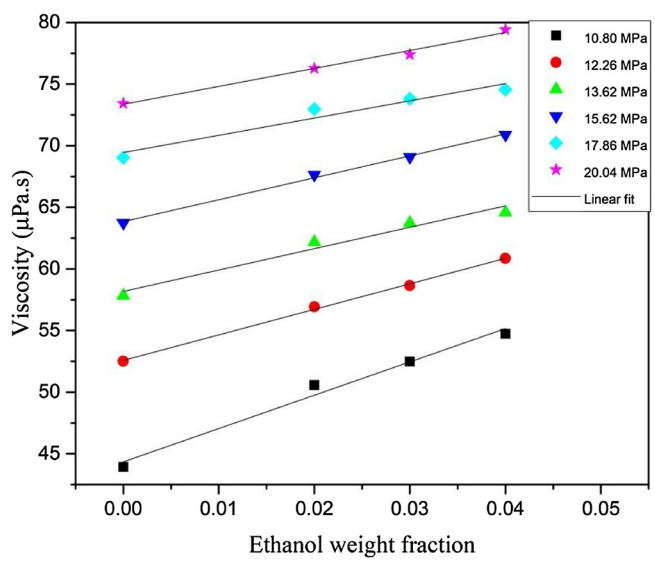

Fig. 5. The dependence of the fluid viscosity, $\boldsymbol{\mu}$, on the ethanol weight fraction, $\boldsymbol{w}$, at different pressures and a fixed temperature of 318 K. Symbols: data points from Tilly et al.[35] ($\boldsymbol{w} \neq 0$) /NIST ($\boldsymbol{w} = 0$), solid lines: linear fits to the data.

the molecules in the mixture become more closely packed and this reduced intermolecular spacing then causes the viscosity to increase [35].

A procedure analogous to that used in deriving Eq. (4) for S_f^m was used to find the composition sensitivity S_Q^m of the cantilever Q-factor from model Eq. (3). The derivative of Q with respect to w (see the details of the derivation in Appendix B) is given as:

$$S_Q^m = \left(\frac{dQ}{dw}\right)_{\boldsymbol{m}} = \frac{1}{\left(\frac{3.8018}{\sqrt{2\mathrm{Re}}} + \frac{2.7364}{2\mathrm{Re}}\right)} \times \left\{ \left[\left(\frac{3.8018Q}{2\sqrt{2\mathrm{Re}}} + \frac{2.7364Q}{2\mathrm{Re}} - \frac{3.7997}{2\sqrt{2\mathrm{Re}}}\right) \left(\frac{1}{\rho} - \frac{1}{\left(\left(\frac{f_{vac}}{f_{fluid}}\right)^2 - \frac{3.7997\pi\rho b}{16\rho_c t\sqrt{2\mathrm{Re}}}\right)} \right.\right.\right.$$
$$\left.\left. \times \left(\frac{1.0553\pi b}{8\rho_c t} + \frac{3.7997\pi b}{16\rho_c t\sqrt{2\mathrm{Re}}}\right)\right) - \frac{4\rho_c t}{\pi\rho^2 b}\right] \frac{\partial\rho}{\partial w}$$
$$\left. - \left[\left(\frac{3.8018Q}{2\sqrt{2\mathrm{Re}}} + \frac{2.7364Q}{2\mathrm{Re}} - \frac{3.7997}{2\sqrt{2\mathrm{Re}}}\right) \left(\frac{1}{\mu} + \frac{1}{\left(\left(\frac{f_{vac}}{f_{fluid}}\right)^2 - \frac{3.7997\pi\rho b}{16\rho_c t\sqrt{2\mathrm{Re}}}\right)} \times \left(\frac{3.7997\pi b\rho}{16\rho_c t\mu\sqrt{2\mathrm{Re}}}\right) \right) \right] \frac{\partial\mu}{\partial w} \right\} \quad (5)$$

Table 2
Derivatives of density and viscosity with respect to the weight fraction of ethanol in the mixture at different fluid pressures and at 318 K. Estimated values of the derivatives are based on the data adopted from [35] and [36].

Pressure (MPa)	$\left(\frac{\partial\rho}{\partial w}\right)$ (kg.m^{-3})	$\left(\frac{\partial\mu}{\partial w}\right)$ (μPa.s)
10.80	2149.16	270.34
12.26	1384.50	207.06
13.62	1055.87	173.43
15.62	788.25	177.79
17.86	604.98	139.82
20.04	445.44	145.59

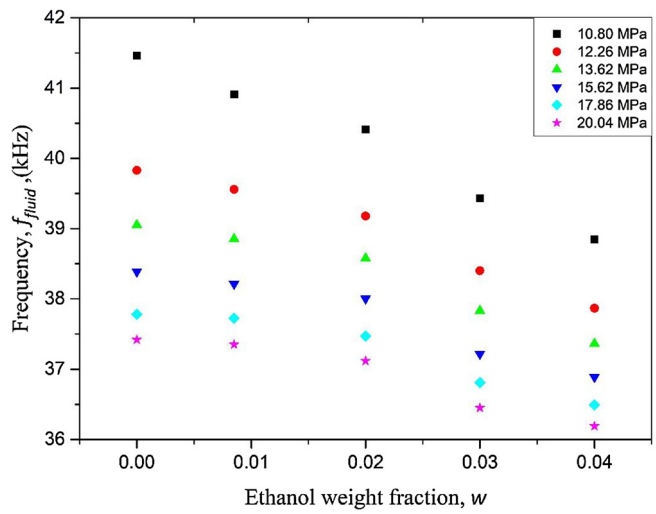

Fig. 6. Variation of the cantilever resonant frequency, f_{fluid}, with ethanol weight fraction, w, at 318 K and different pressures. Microcantilever length: 150 μm.

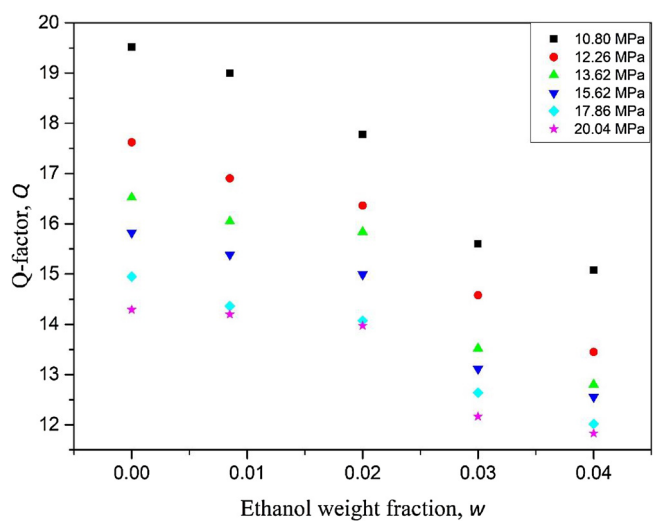

Fig. 7. Variation of the cantilever Q-factor, Q, with ethanol weight fraction, w, at 318 K and different pressures. Microcantilever length: 150 μm.

The sensitivity, S_Q^m, depends on the cantilever parameters f_{vac}, $\rho_c t$, b, cantilever Q-factor, and density and viscosity of the mixture. In addition, the derivatives of density and viscosity with respect to the weight fraction of ethanol in the mixture, $\left(\frac{\partial\rho}{\partial w}\right)$, $\left(\frac{\partial\mu}{\partial w}\right)$, are needed to evaluate S_Q^m at a given experimental condition (pressure, temperature, and composition of the mixture).

In order to characterize the performance of our cantilever-based sensors and determine the model sensitivity of composition measurement, the resonant frequencies f_{fluid} and the Q-factors Q of uncoated microcantilevers of two different lengths (150 μm and 200 μm) immersed in ethanol–CO_2 mixtures within the composition range $w = 0 - 0.04$ were measured at 318 K and pressures varying between 10 MPa to 21 MPa. As could be already inferred from model Eqs. (2) and (3), in connection with the compositional dependence of the mixture density and viscosity illustrated by Figs. 4 and 5, the values of f_{fluid} and Q were observed to change monotonically with w at a particular temperature and pressure. The measured values of f_{fluid} and Q for the two studied cantilevers as a function of w are presented in Figs. 6–9. Using these values, the model sensitivities S_f^m and S_Q^m can be calculated at the particular experimental conditions. For completeness, we

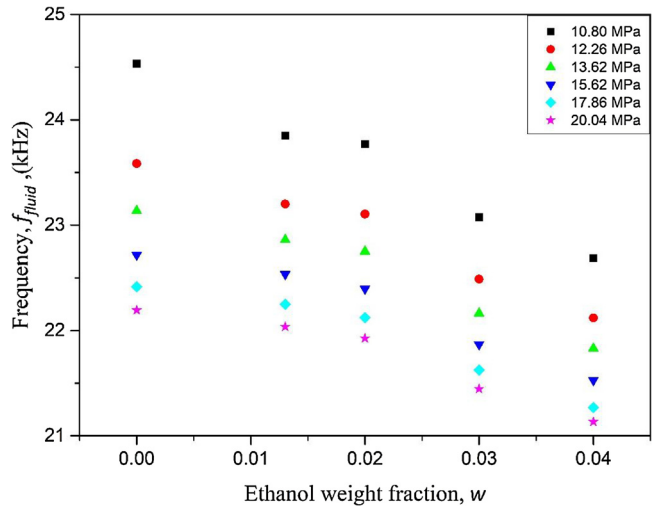

Fig. 8. Variation of the cantilever resonant frequency, f_{fluid}, with ethanol weight fraction, w, at 318 K and different pressures. Microcantilever length: 200 μm.

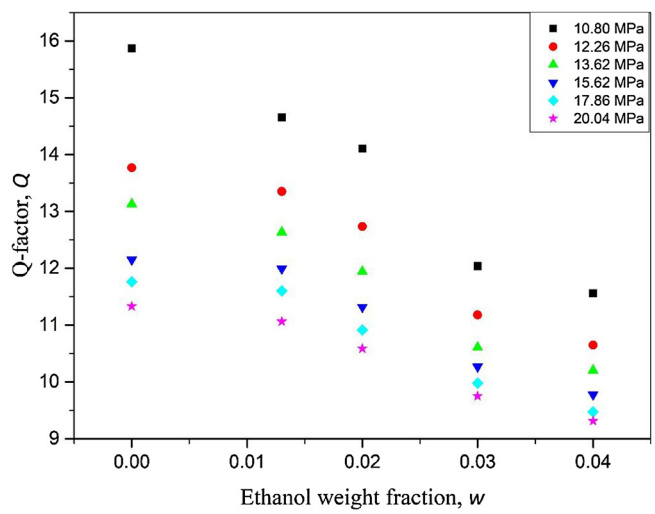

Fig. 9. Variation of the cantilever Q-factor, Q, with ethanol weight fraction, w, at 318 K and different pressures. Microcantilever length: 200 μm.

Table 3
Cantilever parameters for the studied microcantilevers of length 150 μm and 200 μm.

Cantilever parameters	Cantilever length 150 μm	Cantilever length 200 μm
$\rho_c t$(kg/m^2)	0.01375	0.01540
f_{vac} (Hz)	56162	32206
b (μm)	22.66	21.21

also illustrate the change in the cantilever resonant frequency and Q-factor with pressure for different w and the two studied cantilever lengths in Figs. S1-S4 provided in "Supplementary material".

In order to calculate the model sensitivities S_f^m and S_Q^m at a particular temperature and pressure, the cantilever-related parameters (f_{vac}, $\rho_c t$, b) are also required, in addition to the estimates of composition derivatives of mixture density and viscosity provided in Table 2. The necessary cantilever characteristics were obtained using the technique described in our previous study [2]. Briefly, (f_{vac}, $\rho_c t$, b) were regressed from the resonant frequency and Q-factor data recorded with cantilevers immersed in pure CO_2 at a temperature of 318 K and pressure range between 1 MPa and 21 MPa. In particular, the values of (f_{vac}, $\rho_c t$, b) were obtained by minimizing the objective function F (Eq. (6)), using the experimental values of the cantilever resonant frequency, $f_{fluid,i}$ and Q-factor, Q_i measured in pure CO_2 and the density and viscosity of CO_2 at the given experimental pressure and temperature determined from the NIST Chemistry webbook [36]:

$$F = \sum_i \left\{ \left(f_{fluid,i} - f_{vac} \left[1 + \frac{\pi\rho b}{4\rho_c t} \left(1.0553 + 3.7997 \sqrt{\frac{2\mu}{\rho 2\pi f_{fluid,i} b^2}} \right) \right]^{-1/2} \right)^2 + \left(Q_i - \frac{\frac{4\rho_c t}{\pi\rho b} + (1.0553 + 3.7997 \sqrt{\frac{2\mu}{\rho 2\pi f_{fluid,i} b^2}})}{3.8018 \sqrt{\frac{2\mu}{\rho 2\pi f_{fluid,i} b^2}} + 2.7364 \frac{2\mu}{\rho 2\pi f_{fluid,i} b^2}} \right)^2 \right\} \quad (6)$$

Here, the summation index i runs over all experimental values of $f_{fluid,i}$ and Q_i recorded for pure CO_2 at varying pressures. The resulting cantilever parameters are given in Table 3 for the microcantilevers of the length of 150 μm and 200 μm.

Table 4
Contribution of the density and viscous terms to the model sensitivity $\boldsymbol{S_f^m}(\boldsymbol{w} = 0.04)$ (Hz) for the microcantilevers of length 150 μm.

Pressure (MPa)	*Density term (DT)	**Viscous term (VT)	$S_f^m(w = 0.04)$	***VTC contribution to model sensitivity (%)
10.80	−29474.00	−2781.20	−32255.20	8.62
12.26	−17628.00	−1964.00	−19592.00	10.02
13.62	−12931.00	−1575.90	−14506.90	10.86
15.62	−9318.70	−1525.90	−10844.60	14.07
17.86	−6932.90	−1158.50	−8091.40	14.32
20.04	−4989.70	−1159.00	−6148.70	18.85

* Density term (DT) $= -\frac{1}{((\frac{f_{vac}}{f_{fluid}})^3 - \frac{3.7997\pi\rho b f_{vac}}{16 f_{fluid}\rho_c t\sqrt{2\mathrm{Re}}})} \times \{(\frac{1.0553\pi b f_{vac}}{8\rho_c t} + \frac{3.7997\pi b f_{vac}}{16\rho_c t\sqrt{2\mathrm{Re}}})\frac{\partial\rho}{\partial w}\}$.

** Viscous term (VT) $= -\frac{1}{((\frac{f_{vac}}{f_{fluid}})^3 - \frac{3.7997\pi\rho b f_{vac}}{16 f_{fluid}\rho_c t\sqrt{2\mathrm{Re}}})} \times \{(\frac{3.7997\pi b f_{vac}\rho}{16\mu\rho_c t\sqrt{2\mathrm{Re}}})\frac{\partial\mu}{\partial w}\}$.

*** **Viscous term contribution (VTC)** $= \frac{\mathbf{VT}}{\mathrm{DT+VT}}$.

Table 5
Contribution of the density and viscous terms to the model sensitivity $\boldsymbol{S_f^m}(\boldsymbol{w} = 0.04)$ (Hz) for the microcantilevers of length 200 μm.

Pressure (MPa)	*Density term (DT)	**Viscous term (VT)	$S_f^m(w = 0.04)$	***VTC contribution to model sensitivity (%)
10.80	−15319.00	−1973.20	−17292.20	11.41
12.26	−9182.40	−1395.30	−10577.70	13.19
13.62	−6744.20	−1120.40	−7864.60	14.25
15.62	−4846.70	−1081.70	−5928.40	18.25
17.86	−3593.30	−818.59	−4411.89	18.55
20.04	−2603.00	−823.04	−3426.04	24.02

Table 6
Model sensitivity $\boldsymbol{S_f^m}$ (Hz) calculated using Eq. (4) for the microcantilever of length 150 μm.

Pressure (MPa)	$S_f^m(w = 0.04)$	$S_f^m(w = 0.03)$	$S_f^m(w = 0.02)$	$S_f^m(w = 0)$
10.80	−32255.20	−33683.50	−36220.40	−39032.50
12.26	−19592.00	−20414.80	−21664.00	−22732.00
13.62	−14506.90	−15044.50	−15944.60	−16526.30
15.62	−10844.60	−11133.10	−11843.00	−12205.70
17.86	−8091.40	−8299.30	−8743.10	−8967.60
20.04	−6148.70	−6284.20	−6629.20	−6794.60

Table 7
Model sensitivity $\boldsymbol{S_Q^m}$ calculated using Eq. (5) for the microcantilever of length 150 μm.

Pressure (MPa)	$S_Q^m(w = 0.04)$	$S_Q^m(w = 0.03)$	$S_Q^m(w = 0.02)$	$S_Q^m(w = 0)$
10.80	−44.70	−48.46	−54.73	−69.58
12.26	−26.96	−29.64	−33.04	−38.43
13.62	−19.92	−21.04	−23.95	−26.98
15.62	−17.20	−18.32	−20.74	−23.16
17.86	−12.28	−12.91	−14.20	−15.83
20.04	−11.36	−11.96	−13.65	−14.52

Model sensitivities S_f^m and S_Q^m defined by Eqs. (4) and (5) consist of a density term (DT) formed by the compositional derivative of density $\frac{\partial\rho}{\partial w}$ with its pre-factor and a viscous term (VT) given by the compositional derivative of viscosity $\frac{\partial\mu}{\partial w}$ with its pre-factor. Tables 4 and 5 summarize the contribution of DT and VT to the sensitivity S_f^m calculated using Eq. (4) for ethanol weight fraction $w = 0.04$ and microcantilevers of 150 μm and 200 μm lengths, respectively. Evaluation of Eq. (4) for our particular cantilever and fluid characteristics at the studied fluid temperature and pressure shows that VT contributes ∼8 to 19% to the value of S_f^m of the 150 μm long cantilever and ∼11 to 24% to the value of S_f^m of the 200 μm long cantilever. In both cases, the viscous-term contribution is significant and its importance further increases with increasing fluid pressure. Therefore, VT should not be neglected in the analysis of the compositional sensitivity of cantilever-based measurements, especially when they are carried out with high-pressure fluid mixtures. The same conclusions can be drawn for other studied ethanol weight fractions $w = 0$, 0.02 and 0.03 (data not shown). A similar analysis can be carried out for the model sensitivity S_Q^m defined by Eq. (5). In this case, the contribution of VT is dominant in the overall value of S_Q^m, which results from the strong dependence of the Q-factor on the dissipation in the fluid and, thus, the fluid viscosity. In particular, over the studied pressure range, VT contributes ∼81 to 92% to the value of S_Q^m for the 150 μm long cantilever and ∼77 to 91% to the value of S_Q^m for the 200 μm long cantilever.

Tables 6–9 summarize the sensitivities S_f^m and S_Q^m calculated for ethanol weight fractions of 0.04, 0.03, 0.02, and 0 using the data summarized in Tables 2 and 3 and Figs. 4–9. From Tables 6–9, it is evident that at a given pressure, temperature, and composition, microcantilevers of length 150 μm exhibit higher values of S_f^m and S_Q^m in comparison to microcantilevers of length 200 μm. This higher sensitivity of shorter cantilevers is a direct consequence of their higher resonant frequency and higher Q-factor. For both cantilever lengths, the sensitivity values decrease with increasing pressure; this is caused by a monotonic increase of the density and viscosity of the fluid mixture with increasing pressure, which subsequently leads to the reduction of f_{fluid} and Q. At a particular temperature and pressure, sensitivity values change with composition in a nonlinear fashion, following the nonlinear dependence of f_{fluid} and Q on the ethanol

Table 8
Model sensitivity S_f^m (Hz) calculated using Eq. (4) for the microcantilever of length 200 μm.

Pressure (MPa)	$S_f^m(w = 0.04)$	$S_f^m(w = 0.03)$	$S_f^m(w = 0.02)$	$S_f^m(w = 0)$
10.80	−17292.20	−18166.40	−19819.90	−21734.40
12.26	−10577.70	−11102.00	−12018.30	−12759.00
13.62	−7864.60	−8218.30	−8872.30	−9319.90
15.62	−5928.40	−6208.00	−6658.50	−6944.80
17.86	−4411.89	−4629.44	−4946.85	−5148.16
20.04	−3426.04	−3578.66	−3818.53	−3959.43

Table 9
Model sensitivity S_Q^m calculated using Eq. (5) for the microcantilever of length 200 μm.

Pressure (MPa)	$S_Q^m(w = 0.04)$	$S_Q^m(w = 0.03)$	$S_Q^m(w = 0.02)$	$S_Q^m(w = 0)$
10.80	−35.85	−39.03	−44.62	−57.59
12.26	−21.84	−23.63	−26.56	−31.01
13.62	−16.16	−16.94	−18.85	−21.93
15.62	−13.66	−14.63	−16.13	−18.25
17.86	−9.82	−10.36	−11.26	−12.69
20.04	−9.02	−9.66	−10.54	−11.64

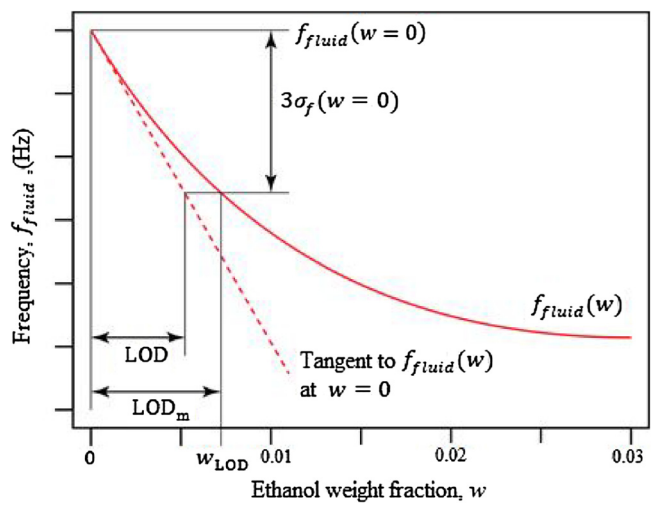

Fig. 10. Illustration of determination of the Limit of Detection (LOD).

concentration in the mixture, w. In general, both S_f^m and S_Q^m – or more precisely, their absolute values – increase with decreasing w. This trend then implies a better resolution of composition measurements carried out in low-concentration mixtures and it has a direct consequence for the achievable limit of detection of cantilever-based sensing.

Limit of Detection (LOD) is the lowest quantity of an analyte that can be distinguished from the blank sample value with a sufficient confidence. In our case, LOD is the smallest ethanol weight fraction in the mixture that can be unambiguously detected. In the literature, different methods can be found to estimate the LOD depending on the complexity of the data obtained from the analytical system and the relationship between the experimentally measured parameter and the actual quantity of interest [37–49]. Two of these approaches for LOD estimation are illustrated in Fig. 10. For the sake of brevity, let us consider only the compositional measurements based on recording the cantilever resonant frequency f_{fluid} ; LOD estimation from the Q-factor measurements can be carried out in an analogous manner. The most rigorous method makes direct use of the known functional relationship between f_{fluid} and the mixture composition w. This non-linear function $f_{fluid} = f_{fluid}(w)$ can be derived using Sader's model Eq. (2), in combination with the reference data [35] on the density and viscosity of ethanol−CO_2 mixtures, and it is schematically illustrated by the solid red curve shown in Fig. 10. From the repeated measurements carried out with pure CO_2, we know the values of $f_{fluid}(w = 0)$ and also the standard deviations of the measurements of f_{fluid} at $w = 0$, $\sigma_f(w = 0)$ that quantify the precision with which f_{fluid} can be measured. Assuming we can distinguish with confidence greater than 99.6% the values of f_{fluid} that are separated by $\pm 3\sigma_f$, we can calculate the resonant frequency $f_{fluid}\,(w = w_{\text{LOD}})$ for the minimum detectable weight fraction of ethanol w_{LOD} as:

$$f_{fluid}\,(w = w_{\text{LOD}}) = \left[f_{fluid}\,(w = 0) - 3\sigma_f(w = 0)\right] \tag{7}$$

Subsequently, we can use the known functional relationship $f_{fluid} = f_{fluid}(w)$ to find the actual value of w_{LOD} corresponding to $f_{fluid}\,(w = w_{\text{LOD}})$; w_{LOD} is then precisely equal to the true LOD indicated as LOD_{m} in Fig. 10. Alternatively, we can approximate the nonlinear function $f_{fluid} = f_{fluid}(w)$ in a small neighborhood of the point $w = 0$ with a line, following the approach based on IUPAC recommendation [50] and discussed in detail by Ramos et al. [37]. This linear approximation is illustrated in Fig. 10 by the dashed line which forms a tangent

Table 10
Limit of detection LOD_f of microcantilever-based measurements at 318 K and different pressures. (a) Microcantilever length: 150 μm and (b) Microcantilever length: 200 μm.

(a)						
Pressure (MPa)	10.80	12.26	13.62	15.62	17.86	20.04
Standard deviation σ_f (Hz)	11.58	11.21	17.44	12.35	6.35	16.14
$S_f^m(w=0)$	−39032.50	−22732.00	−16526.30	−12205.70	−8967.60	−6794.60
LOD_f (ethanol wt fraction)	0.0009	0.0015	0.0032	0.0030	0.0021	0.0071
(b)						
Pressure (MPa)	10.80	12.26	13.62	15.62	17.86	20.04
Standard deviation σ_f (Hz)	13.24	20.86	13.42	21.85	12.17	16.00
$S_f^m(w=0)$	−21734.40	−12759.00	−9319.90	−6944.80	−5148.16	−3959.43
LOD_f (ethanol wt fraction)	0.0018	0.0049	0.0043	0.0094	0.0071	0.0121

Table 11
Limit of detection LOD_Q of microcantilever-based measurements at 318 K and different pressures. (a) Microcantilever length: 150 μm and (b) Microcantilever length: 200 μm.

(a)						
Pressure (MPa)	10.80	12.26	13.62	15.62	17.86	20.04
Standard deviation σ_Q	0.10	0.13	0.15	0.11	0.11	0.10
$S_Q^m(w=0)$	−69.58	−38.43	−26.98	−23.16	−15.83	−14.52
LOD_Q (ethanol wt fraction)	0.0043	0.0101	0.0172	0.0147	0.0206	0.0215
(b)						
Pressure (MPa)	10.80	12.26	13.62	15.62	17.86	20.04
Standard deviation σ_Q	0.19	0.02	0.10	0.12	0.13	0.08
$S_Q^m(w=0)$	−57.59	−31.01	−21.93	−18.25	−12.69	−11.64
LOD_Q (ethanol wt fraction)	0.0100	0.0019	0.0135	0.0201	0.0298	0.0213

to the graph of $f_{fluid} = f_{fluid}(w)$ at $= 0$, with a slope S that corresponds to the sensitivity df_{fluid}/dw evaluated at $w = 0$. Within the linear approximation, the LOD can be estimated as:

$$\mathrm{LOD} = \frac{k_d \sigma_b}{S} \tag{8}$$

Here, σ_b is the standard deviation of the blank (sample with $w = 0$) and k_d is a number that is chosen according to the desired confidence level. As mentioned above, $k_d = 3$ implies 99.6% confidence level and it is strongly recommended. Consequently, in our particular case, LOD can be defined as:

$$\mathrm{LOD}_f = \frac{3\sigma_f}{S_f^m(w=0)} \tag{9}$$

$$\mathrm{LOD}_Q = \frac{3\sigma_Q}{S_Q^m(w=0)} \tag{10}$$

where σ_f and σ_Q are the standard deviations of the resonant frequency and the Q-factor of the cantilevers measured in pure CO_2 ($w = 0$) and the values of $S_f^m(w=0)$ and $S_Q^m(w=0)$ are obtained using Eqs. (4) and (5). For the purpose of calculating LOD, absolute values of sensitivities are used.

Tables 10 and 11 summarize the numerical values of LOD_f and LOD_Q calculated from Eqs. (9) and (10) using the standard deviations of the resonant frequency and the Q-factor of microcantilevers immersed in pure CO_2 at different pressures. For the purpose of LOD calculations, the values of $S_f^m(w=0)$ and $S_Q^m(w=0)$ for the 150 μm and 200 μm long microcantilevers were taken from Tables 6–9. The comparison of Tables 10(a) and 11(a) shows that the minimum detectable weight fraction of ethanol determined from the measurement of f_{fluid} and Q at the pressure of 10.8 MPa with the 150 μm long cantilever was 0.0009 and 0.0043, respectively. Similarly, for the 200 μm long cantilever at the same pressure, the minimum detectable ethanol weight fraction determined from the measurement of f_{fluid} and Q was 0.0018 and 0.0100, respectively (compare Tables 10(b) and 11(b)). A similar relationship between LOD_f and LOD_Q was observed at all studied pressures.

From the above comparison of the values of LOD_f and LOD_Q, it is clear that the resonant frequency is a more sensitive indicator for measuring the mixture composition at an arbitrary fluid pressure. Thus, the model sensitivity S_f^m given by Eq. (4) can be used to find the true LOD of ethanol in ethanol−CO_2 mixtures. Since LOD also depends on the standard deviation of the measurements of f_{fluid}, the stability of the resonant frequency during the measurement and the precision of its determination are important. The LOD analysis shows that the shorter 150 μm cantilever has a higher measurement sensitivity and, hence, a lower achievable LOD. Therefore, short-length cantilevers are suggested for high-resolution micro-sensing of the composition of fluid mixtures.

4. Conclusion

We have studied the sensitivity of cantilever-based measurement of composition of ethanol−CO_2 mixtures at 318 K and pressure range between 10 MPa to 21 MPa. To this end, we have derived analytical expressions quantifying the change in the resonant frequency and

the Q-factor of an immersed cantilever with the ethanol weight fraction in the mixture. We have calculated the effect of viscous term on the sensitivity of compositional measurements and shown that its contribution is significant and cannot be neglected in the analysis. In general, the importance of viscous term is higher at higher pressures. Using our model sensitivity formulas and the standard deviations of the resonant frequency and the Q-factor determined from repeated measurements of the cantilever frequency response at a particular condition, we have estimated the minimum weight fractions of ethanol LOD_f and LOD_Q that can be detected in ethanol–CO_2 mixtures at various pressures. We have demonstrated that the cantilever resonant frequency is a more sensitive indicator of the composition of fluid mixtures as compared to the Q-factor. In particular, the minimum weight fraction of ethanol that can be detected with the current setup with a 150 μm long cantilever is between 0.0009 and 0.0071 in the pressure range of 10 MPa to 21 MPa.

Our study represents the first attempt to derive rigorous analytical expressions which relate the change in the cantilever resonant frequency and Q-factor to the mixture composition. We have used ethanol–CO_2 mixtures as the model fluid to analyze the sensitivity of microcantilever-based compositional measurements; however, our method can be readily extended to other fluid mixtures. Thus, it can find possible applications in technological processes ranging from the synthesis of nanostructured materials to the fabrication of various functional microdevices.

Acknowledgments

This project has received funding from the European Unionś Horizon 2020 research and innovation programme under grant agreement No 685648. We gratefully acknowledge Ummu Koc and Mahmut Bicer for the fabrication of the microcantilevers.

Appendix A. Derivation of formula for the sensitivity $S_f = \left(\frac{df_{fluid}}{dw}\right)$

Using Sader's model [16] of cantilever oscillations in a viscous fluid combined with Maali's analytical approximation [34], the cantilever resonant frequency f_{fluid} is given as:

$$f_{fluid} = f_{vac}\left[1 + \frac{\pi\rho b}{4\rho_c t}\left(1.0553 + 3.7997\sqrt{\frac{2\mu}{\rho 2\pi f_{fluid} b^2}}\right)\right]^{-1/2} \tag{A1}$$

Eq. (A1) defines f_{fluid} as an implicit function of the fluid parameters $\rho,\ \mu$ that themselves depend on the mixture composition w. Let us introduce formally an implicit function $h\left(f_{fluid}, \rho,\ \mu\right)$ as:

$$h\left(f_{fluid}, \rho,\ \mu\right) = f_{fluid} - f_{vac}\left[1 + \frac{\pi\rho b}{4\rho_c t}\left(1.0553 + 3.7997\sqrt{\frac{2\mu}{\rho 2\pi f_{fluid} b^2}}\right)\right]^{-1/2} = 0 \tag{A2}$$

The total differential of $h\left(f_{fluid}, \rho,\ \mu\right)$ with respect to its variables then has the form

$$dh = \frac{\partial h}{\partial \rho}d\rho + \frac{\partial h}{\partial \mu}d\mu + \frac{\partial h}{\partial f_{fluid}}df_{fluid} = 0 \tag{A3}$$

The derivative of $h\left(f_{fluid}, \rho,\ \mu\right)$ with respect to ρ reads as:

$$\frac{\partial h}{\partial \rho} = \frac{f_{vac}}{2}\left[1 + \frac{\pi\rho b}{4\rho_c t}\left(1.0553 + 3.7997\sqrt{\frac{2\mu}{\rho 2\pi f_{fluid} b^2}}\right)\right]^{-3/2}\left[\frac{1.0553\pi b}{4\rho_c t} + \frac{3.7997\pi b}{8\rho_c t}\sqrt{\frac{2\mu}{\rho 2\pi f_{fluid} b^2}}\right] \tag{A4}$$

Using Eq. (A1), expression (A4) can be further simplified as:

$$\frac{\partial h}{\partial \rho} = \frac{f_{vac}}{2}\left(\frac{f_{fluid}}{f_{vac}}\right)^3\left(\frac{1.0553\pi b}{4\rho_c t} + \frac{3.7997\pi b}{8\rho_c t}\sqrt{\frac{2\mu}{\rho 2\pi f_{fluid} b^2}}\right) \tag{A5}$$

The derivative of $h\left(f_{fluid}, \rho,\ \mu\right)$ with respect to μ reads as:

$$\frac{\partial h}{\partial \mu} = \frac{f_{vac}}{2}\left[1 + \frac{\pi\rho b}{4\rho_c t}\left(1.0553 + 3.7997\sqrt{\frac{2\mu}{\rho 2\pi f_{fluid} b^2}}\right)\right]^{-3/2}\left(\frac{3.7997\pi b\rho}{8\rho_c t\sqrt{\mu}}\sqrt{\frac{2}{\rho 2\pi f_{fluid} b^2}}\right), \tag{A6}$$

which, after further simplification using Eq. (A1), transforms to:

$$\frac{\partial h}{\partial \mu} = \frac{f_{vac}}{2}\left(\frac{f_{fluid}}{f_{vac}}\right)^3\left(\frac{3.7997\pi b\rho}{8\rho_c t}\sqrt{\frac{2}{\rho\mu 2\pi f_{fluid} b^2}}\right) \tag{A7}$$

Finally, taking the derivative of $h\left(f_{fluid}, \rho,\ \mu\right)$ with respect to f_{fluid}, we obtain:

$$\frac{\partial h}{\partial f_{fluid}} = 1 + \frac{f_{vac}}{2}\left[1 + \frac{\pi\rho b}{4\rho_c t}\left(1.0553 + 3.7997\sqrt{\frac{2\mu}{\rho 2\pi f_{fluid} b^2}}\right)\right]^{-3/2}\left(-\frac{3.7997\pi\rho b}{8 f_{fluid}\sqrt{f_{fluid}}\rho_c t}\sqrt{\frac{2\mu}{\rho 2\pi b^2}}\right), \tag{A8}$$

which can be again simplified to

$$\frac{\partial h}{\partial f_{fluid}} = 1 - \frac{f_{vac}}{2}\left(\frac{f_{fluid}}{f_{vac}}\right)^3\left(\frac{3.7997\pi\rho b}{8 f_{fluid}\rho_c t}\sqrt{\frac{2\mu}{\rho 2\pi f_{fluid} b^2}}\right) \tag{A9}$$

Inserting Eqs. (A5), (A7), and (A9) into formula (A3) then gives:

$$dh = \frac{f_{vac}}{2}\left(\frac{f_{fluid}}{f_{vac}}\right)^3\left(\frac{1.0553\pi b}{4\rho_c t} + \frac{3.7997\pi b}{8\rho_c t}\sqrt{\frac{2\mu}{\rho 2\pi f_{fluid} b^2}}\right)d\rho + \frac{f_{vac}}{2}\left(\frac{f_{fluid}}{f_{vac}}\right)^3\left(\frac{3.7997\pi b\rho}{8\rho_c t}\sqrt{\frac{2}{\rho\mu 2\pi f_{fluid} b^2}}\right)d\mu$$
$$+\left(1-\frac{f_{vac}}{2}\left(\frac{f_{fluid}}{f_{vac}}\right)^3\left(\frac{3.7997\pi\rho b}{8 f_{fluid}\rho_c t}\sqrt{\frac{2\mu}{\rho 2\pi f_{fluid} b^2}}\right)\right)df_{fluid} = 0 \tag{A10}$$

Upon substituting for the Reynolds number $\mathrm{Re} = \left(2\pi f_{fluid}\rho b^2\right)/(4\mu)$ and expressing the differential df_{fluid} as a function of differentials $d\rho,\ d\mu$, Eq. (A10) is transformed into

$$\left(\left(\frac{f_{vac}}{f_{fluid}}\right)^3 - \frac{3.7997\pi\rho b f_{vac}}{16 f_{fluid}\rho_c t\sqrt{2\mathrm{Re}}}\right)df_{fluid} =$$
$$= -\left(\frac{1.0553\pi b f_{vac}}{8\rho_c t} + \frac{3.7997\pi b f_{vac}}{16\rho_c t\sqrt{2\mathrm{Re}}}\right)d\rho - \left(\frac{3.7997\pi b\rho f_{vac}}{16\rho_c t\mu\sqrt{2\mathrm{Re}}}\right)d\mu \tag{A11}$$

By applying the chain rule, we can introduce the derivatives of individual parameters $\left(f_{fluid},\ \rho,\ \mu\right)$ with respect to the ethanol weight fraction (mixture composition) w:

$$\left(\left(\frac{f_{vac}}{f_{fluid}}\right)^3 - \frac{3.7997\pi\rho b f_{vac}}{16 f_{fluid}\rho_c t\sqrt{2Re}}\right)df_{fluid} = -\left(\frac{1.0553\pi b f_{vac}}{8\rho_c t} + \frac{3.7997\pi b f_{vac}}{16\rho_c t\sqrt{2\mathrm{Re}}}\right)\frac{\partial\rho}{\partial w}dw - \left(\frac{3.7997\pi b\rho f_{vac}}{16\rho_c t\mu\sqrt{2\mathrm{Re}}}\right)\frac{\partial\mu}{\partial w}dw \tag{A12}$$

or

$$\left(\left(\frac{f_{vac}}{f_{fluid}}\right)^3 - \frac{3.7997\pi\rho b f_{vac}}{16 f_{fluid}\rho_c t\sqrt{2\mathrm{Re}}}\right)\frac{df_{fluid}}{dw} = -\left(\frac{1.0553\pi b f_{vac}}{8\rho_c t} + \frac{3.7997\pi b f_{vac}}{16\rho_c t\sqrt{2\mathrm{Re}}}\right)\frac{\partial\rho}{\partial w} - \left(\frac{3.7997\pi b\rho f_{vac}}{16\rho_c t\mu\sqrt{2Re}}\right)\frac{\partial\mu}{\partial w} \tag{A13}$$

Final rearrangement of formula (A13) gives the sensitivity S_f:

$$S_f = \frac{df_{fluid}}{dw} = \frac{1}{\left(\left(\frac{f_{vac}}{f_{fluid}}\right)^3 - \frac{3.7997\pi\rho b f_{vac}}{16 f_{fluid}\rho_c t\sqrt{2\mathrm{Re}}}\right)} \times \left\{-\left(\frac{1.0553\pi b f_{vac}}{8\rho_c t} + \frac{3.7997\pi b f_{vac}}{16\rho_c t\sqrt{2\mathrm{Re}}}\right)\frac{\partial\rho}{\partial w} - \left(\frac{3.7997\pi b\rho f_{vac}}{16\rho_c t\mu\sqrt{2\mathrm{Re}}}\right)\frac{\partial\mu}{\partial w}\right\} \tag{A14}$$

Appendix B. Derivation of formula for the sensitivity $S_Q = \left(\frac{dQ}{dw}\right)$

Sader's model [16] equation for the cantilever Q-factor Q in Maali's analytical approximation [34] is given by:

$$Q = \frac{\frac{4\rho_c t}{\pi\rho b} + \left(1.0553 + 3.7997\sqrt{\frac{2\mu}{\rho 2\pi f_{fluid} b^2}}\right)}{3.8018\sqrt{\frac{2\mu}{\rho 2\pi f_{fluid} b^2}} + 2.7364\frac{2\mu}{\rho 2\pi f_{fluid} b^2}} \tag{B1}$$

Eq. (B1) defines Q as a function of the fluid parameters ρ and μ, and the cantilever resonant frequency f_{fluid}. Following the same approach as used in deriving the sensitivity S_f, let us introduce an implicit function $g\left(Q, f_{fluid},\ \rho,\ \mu\right)$:

$$g = Q\times 3.8018\sqrt{\frac{2\mu}{\rho 2\pi f_{fluid} b^2}} + Q\times 2.7364\frac{2\mu}{\rho 2\pi f_{fluid} b^2} - \frac{4\rho_c t}{\pi\rho b} - \left(1.0553 + 3.7997\sqrt{\frac{2\mu}{\rho 2\pi f_{fluid} b^2}}\right) = 0 \tag{B2}$$

with the total differential

$$dg = \frac{\partial g}{\partial Q}dQ + \frac{\partial g}{\partial f_{fluid}}df_{fluid} + \frac{\partial g}{\partial\rho}d\rho + \frac{\partial g}{\partial\mu}d\mu = 0 \tag{B3}$$

Evaluation of the partial derivatives $\frac{\partial g}{\partial Q}$, $\frac{\partial g}{\partial f_{fluid}}$, $\frac{\partial g}{\partial\rho}$, and $\frac{\partial g}{\partial\mu}$ which appear in Eq. (B3) leads to:

$$\left(3.8018\sqrt{\frac{2\mu}{\rho 2\pi f_{fluid} b^2}} + 2.7364\frac{2\mu}{\rho 2\pi f_{fluid} b^2}\right)dQ + \left(-\frac{3.8018Q}{2f_{fluid}}\sqrt{\frac{2\mu}{\rho 2\pi f_{fluid} b^2}} - 2.7364\frac{2\mu Q}{\rho 2\pi {f_{fluid}}^2 b^2} + \frac{3.7997}{2f_{fluid}}\sqrt{\frac{2\mu}{\rho 2\pi f_{fluid} b^2}}\right)df_{fluid}$$
$$+\left(-\frac{3.8018Q}{2\rho}\sqrt{\frac{2\mu}{\rho 2\pi f_{fluid} b^2}} - 2.7364\frac{2\mu Q}{\rho^2 2\pi f_{fluid} b^2} + \frac{4\rho_c t}{\pi\rho^2 b} + \frac{3.7997}{2\rho}\sqrt{\frac{2\mu}{\rho 2\pi f_{fluid} b^2}}\right)d\rho$$
$$+\left(\frac{3.8018Q}{2}\sqrt{\frac{2}{\rho\mu 2\pi f_{fluid} b^2}} + 2.7364\frac{2Q}{\rho 2\pi f_{fluid} b^2} - \frac{3.7997}{2}\sqrt{\frac{2}{\rho\mu 2\pi f_{fluid} b^2}}\right)d\mu = 0 \tag{B4}$$

Substituting for the Reynolds number $\mathrm{Re} = \left(2\pi f_{fluid}\rho b^2\right)/(4\mu)$ and rearranging the terms so that dQ is expressed as a function of $df_{fluid}, d\rho, d\mu$ leads to:

$$\left(\frac{3.8018}{\sqrt{2\mathrm{Re}}} + \frac{2.7364}{2\mathrm{Re}}\right) dQ = \left(\frac{3.8018Q}{2f_{fluid}\sqrt{2\mathrm{Re}}} + \frac{2.7364Q}{2f_{fluid}\mathrm{Re}} - \frac{3.7997}{2f_{fluid}\sqrt{2\mathrm{Re}}}\right) df_{fluid} + \left(\frac{3.8018Q}{2\rho\sqrt{2\mathrm{Re}}} + \frac{2.7364Q}{2\rho\mathrm{Re}} - \frac{4\rho_c t}{\pi\rho^2 b} - \frac{3.7997}{2\rho\sqrt{2\mathrm{Re}}}\right) d\rho - \left(\frac{3.8018Q}{2\mu\sqrt{2\mathrm{Re}}} + \frac{2.7364Q}{2\mu\mathrm{Re}} - \frac{3.7997}{2\mu\sqrt{2\mathrm{Re}}}\right) d\mu \tag{B5}$$

In order to evaluate the changes of the Q-factor Q with changing mixture composition w, we can apply the chain rule:

$$\left(\frac{3.8018}{\sqrt{2\mathrm{Re}}} + \frac{2.7364}{2\mathrm{Re}}\right) dQ = \left(\frac{3.8018Q}{2f_{fluid}\sqrt{2\mathrm{Re}}} + \frac{2.7364Q}{2f_{fluid}\mathrm{Re}} - \frac{3.7997}{2f_{fluid}\sqrt{2\mathrm{Re}}}\right) \frac{\partial f_{fluid}}{\partial w} dw + \left(\frac{3.8018Q}{2\rho\sqrt{2\mathrm{Re}}} + \frac{2.7364Q}{2\rho\mathrm{Re}} - \frac{4\rho_c t}{\pi\rho^2 b} - \frac{3.7997}{2\rho\sqrt{2\mathrm{Re}}}\right) \frac{\partial \rho}{\partial w} dw - \left(\frac{3.8018Q}{2\mu\sqrt{2\mathrm{Re}}} + \frac{2.7364Q}{2\mu\mathrm{Re}} - \frac{3.7997}{2\mu\sqrt{2\mathrm{Re}}}\right) \frac{\partial \mu}{\partial w} dw \tag{B6}$$

which subsequently leads to:

$$\left(\frac{3.8018}{\sqrt{2\mathrm{Re}}} + \frac{2.7364}{2\mathrm{Re}}\right) \frac{dQ}{dw} = \left(\frac{3.8018Q}{2f_{fluid}\sqrt{2\mathrm{Re}}} + \frac{2.7364Q}{2f_{fluid}\mathrm{Re}} - \frac{3.7997}{2f_{fluid}\sqrt{2\mathrm{Re}}}\right) \frac{\partial f_{fluid}}{\partial w} + \left(\frac{3.8018Q}{2\rho\sqrt{2\mathrm{Re}}} + \frac{2.7364Q}{2\rho\mathrm{Re}} - \frac{4\rho_c t}{\pi\rho^2 b} - \frac{3.7997}{2\rho\sqrt{2\mathrm{Re}}}\right) \frac{\partial \rho}{\partial w} - \left(\frac{3.8018Q}{2\mu\sqrt{2\mathrm{Re}}} + \frac{2.7364Q}{2\mu\mathrm{Re}} - \frac{3.7997}{2\mu\sqrt{2\mathrm{Re}}}\right) \frac{\partial \mu}{\partial w} \tag{B7}$$

Substituting for $\partial f_{fluid}/\partial w$ from Eq. (A14) transforms formula (B7) to

$$\begin{aligned}\left(\frac{3.8018}{\sqrt{2\mathrm{Re}}} + \frac{2.7364}{2\mathrm{Re}}\right) \frac{dQ}{dw} = {} & \left(\frac{3.8018Q}{2f_{fluid}\sqrt{2\mathrm{Re}}} + \frac{2.7364Q}{2f_{fluid}\mathrm{Re}} - \frac{3.7997}{2f_{fluid}\sqrt{2\mathrm{Re}}}\right) \\ & \left[-\frac{1}{\left(\left(\frac{f_{vac}}{f_{fluid}}\right)^3 - \frac{3.7997\pi\rho b f_{vac}}{16 f_{fluid}\rho_c t\sqrt{2\mathrm{Re}}}\right)} \times \left(\frac{1.0553\pi b f_{vac}}{8\rho_c t} + \frac{3.7997\pi b f_{vac}}{16\rho_c t\sqrt{2\mathrm{Re}}}\right) \frac{\partial \rho}{\partial w}\right. \\ & \left. - \frac{1}{\left(\left(\frac{f_{vac}}{f_{fluid}}\right)^3 - \frac{3.7997\pi\rho b f_{vac}}{16 f_{fluid}\rho_c t\sqrt{2\mathrm{Re}}}\right)} \times \left(\frac{3.7997\pi b\rho f_{vac}}{16\rho_c t\mu\sqrt{2\mathrm{Re}}}\right) \frac{\partial \mu}{\partial w}\right] \\ & + \left(\frac{3.8018Q}{2\rho\sqrt{2\mathrm{Re}}} + \frac{2.7364Q}{2\rho\mathrm{Re}} - \frac{4\rho_c t}{\pi\rho^2 b} - \frac{3.7997}{2\rho\sqrt{2\mathrm{Re}}}\right) \frac{\partial \rho}{\partial w} - \left(\frac{3.8018Q}{2\mu\sqrt{2\mathrm{Re}}} + \frac{2.7364Q}{2\mu\mathrm{Re}} - \frac{3.7997}{2\mu\sqrt{2\mathrm{Re}}}\right) \frac{\partial \mu}{\partial w}\end{aligned} \tag{B8}$$

In the next step, we can isolate the Q-factor compositional derivative dQ/dw and collect together all the terms that determine the dependence of dQ/dw on the derivative of the fluid density $d\rho/dw$ and the derivative of the fluid viscosity $d\mu/dw$:

$$\begin{aligned}\frac{dQ}{dw} = {} & \frac{1}{\left(\frac{3.8018}{\sqrt{2\mathrm{Re}}} + \frac{2.7364}{2\mathrm{Re}}\right)} \times \left\{\left[\left(\frac{3.8018Q}{2\sqrt{2\mathrm{Re}}} + \frac{2.7364Q}{2\mathrm{Re}} - \frac{3.7997}{2\sqrt{2\mathrm{Re}}}\right)\left(\frac{1}{\rho} - \frac{1}{f_{fluid}} \times \frac{1}{\left(\left(\frac{f_{vac}}{f_{fluid}}\right)^3 - \frac{3.7997\pi\rho b f_{vac}}{16 f_{fluid}\rho_c t\sqrt{2\mathrm{Re}}}\right)}\right.\right. \\ & \left.\times \left(\frac{1.0553\pi b f_{vac}}{8\rho_c t} + \frac{3.7997\pi b f_{vac}}{16\rho_c t\sqrt{2\mathrm{Re}}}\right)\right) - \frac{4\rho_c t}{\pi\rho^2 b}\Bigg] \frac{\partial \rho}{\partial w} \\ & - \left[\left(\frac{3.8018Q}{2\sqrt{2\mathrm{Re}}} + \frac{2.7364Q}{2\mathrm{Re}} - \frac{3.7997}{2\sqrt{2\mathrm{Re}}}\right)\left(\frac{1}{\mu} + \frac{1}{f_{fluid}} \times \frac{1}{\left(\left(\frac{f_{vac}}{f_{fluid}}\right)^3 - \frac{3.7997\pi\rho b f_{vac}}{16 f_{fluid}\rho_c t\sqrt{2\mathrm{Re}}}\right)} \times \left(\frac{3.7997\pi b\rho f_{vac}}{16\rho_c t\mu\sqrt{2\mathrm{Re}}}\right)\right)\right] \frac{\partial \mu}{\partial w}\Bigg\}\end{aligned} \tag{B9}$$

Final rearrangement of formula (B9) for dQ/dw then gives the full model equation for the compositional sensitivity of the cantilever Q-factor S_Q:

$$S_Q = \frac{dQ}{dw} = \frac{1}{\left(\frac{3.8018}{\sqrt{2\mathrm{Re}}} + \frac{2.7364}{2\mathrm{Re}}\right)} \times \left\{ \left[\left(\frac{3.8018Q}{2\sqrt{2\mathrm{Re}}} + \frac{2.7364Q}{2\mathrm{Re}} - \frac{3.7997}{2\sqrt{2\mathrm{Re}}} \right) \left(\frac{1}{\rho} - \frac{1}{\left(\left(\frac{f_{vac}}{f_{fluid}} \right)^2 - \frac{3.7997\pi\rho b}{16\rho_c t\sqrt{2\mathrm{Re}}} \right)} \right.\right.\right.$$
$$\left.\left. \times \left(\frac{1.0553\pi b}{8\rho_c t} + \frac{3.7997\pi b}{16\rho_c t\sqrt{2\mathrm{Re}}} \right) \right) - \frac{4\rho_c t}{\pi\rho^2 b} \right] \frac{\partial\rho}{\partial w}$$
$$\left. - \left[\left(\frac{3.8018Q}{2\sqrt{2\mathrm{Re}}} + \frac{2.7364Q}{2\mathrm{Re}} - \frac{3.7997}{2\sqrt{2\mathrm{Re}}} \right) \left(\frac{1}{\mu} + \frac{1}{\left(\left(\frac{f_{vac}}{f_{fluid}} \right)^2 - \frac{3.7997\pi\rho b}{16\rho_c t\sqrt{2\mathrm{Re}}} \right)} \times \left(\frac{3.7997\pi b\rho}{16\rho_c t\mu\sqrt{2\mathrm{Re}}} \right) \right) \right] \frac{\partial\mu}{\partial w} \right\} \tag{B10}$$

References

[1] G. Eris, A.A. Bozkurt, A. Sunol, A. Jonáš, A. Kiraz, B.E. Alaca, C. Erkey, Determination of viscosity and density of fluids using frequency response of microcantilevers, J. Supercrit. Fluids 105 (2015) 179–185.
[2] G. Eriş, S.K. Baloch, A.A. Bozkurt, A. Jonáš, A. Kiraz, B.E. Alaca, C. Erkey, Characterization of fluid mixtures at high pressures using frequency response of microcantilevers, Sensor Actuat. A: Phys. 261 (2017) 202–209.
[3] E. Uzunlar, B. Beykal, K. Ehrlich, D. Sanli, A. Jonáš, B.E. Alaca, A. Kiraz, H. Urey, C. Erkey, Frequency response of microcantilevers immersed in gaseous, liquid, and supercritical carbon dioxide, J. Supercrit. Fluids 81 (2013) 254–264.
[4] M.T. Boudjiet, J. Bertrand, C. Pellet, I. Dufour, New characterization methods for monitoring small resonant frequency variation: experimental tests in the case of hydrogen detection with uncoated silicon microcantilever-based sensors, Sens. Actuat. B: Chem. 199 (2014) 269–276.
[5] S. Tétin, B. Caillard, F. Ménil, H. Debéda, C. Lucat, C. Pellet, I. Dufour, Modeling and performance of uncoated microcantilever-based chemical sensors, Sens. Actuat. B: Chem. 143 (2010) 555–560.
[6] M.T. Boudjiet, V. Cuisset, C. Pellet, J. Bertrand, I. Dufour, Preliminary results of the feasibility of hydrogen detection by the use of uncoated silicon microcantilever-based sensors, Int. J. Hydrogen Energy 39 (2014) 20497–20502.
[7] M.-T. Boudjiet, J. Bertrand, F. Mathieu, L. Nicu, L. Mazenq, T. Leïchlé, S.M. Heinrich, C. Pellet, I. Dufour, Geometry optimization of uncoated silicon microcantilever-based gas density sensors, Sens. Actuat.B: Chem. 208 (2015) 600–607.
[8] O. Cakmak, E. Ermek, N. Kilinc, G.G. Yaralioglu, H. Urey, Precision density and viscosity measurement using two cantilevers with different widths, Sens. Actuat. A: Phys. 232 (2015) 141–147.
[9] M. Youssry, N. Belmiloud, B. Caillard, C. Ayela, C. Pellet, I. Dufour, A straightforward determination of fluid viscosity and density using microcantilevers: from experimental data to analytical expressions, Sensor Actuat. A: Phys. 172 (2011) 40–46.
[10] I. Dufour, E. Lemaire, B. Caillard, H. Debéda, C. Lucat, S.M. Heinrich, F. Josse, O. Brand, Effect of hydrodynamic force on microcantilever vibrations: applications to liquid-phase chemical sensing, Sens. Actuators B: Chem. 192 (2014) 664–672.
[11] T. Manzaneque, V. Ruiz-Díez, J. Hernando-García, E. Wistrela, M. Kucera, U. Schmid, J.L. Sánchez-Rojas, Piezoelectric MEMS resonator-based oscillator for density and viscosity sensing, Sensor Actuat. A: Phys. 220 (2014) 305–315.
[12] E. Lemaire, B. Caillard, M. Youssry, I. Dufour, High-frequency viscoelastic measurements of fluids based on microcantilever sensing: New modeling and experimental issues, Sensor Actuat. A: Phys. 201 (2013) 230–240.
[13] B.A. Bircher, L. Duempelmann, K. Renggli, H.P. Lang, C. Gerber, N. Bruns, T. Braun, Real-time viscosity and mass density sensors requiring microliter sample volume based on nanomechanical resonators, Anal. Chem. 85 (2013) 8676–8683.
[14] S.K. Baloch, A. Jonáš, A. Kiraz, B.E. Alaca, C. Erkey, Determination of composition of ethanol-CO2 mixtures at high pressures using frequency response of microcantilevers, The J. Supercrit. Fluids 132 (2018) 65–70.
[15] K.M. Goeders, J.S. Colton, L.A. Bottomley, Microcantilevers: sensing chemical interactions via mechanical motion, Chem. Rev. 108 (2008) 522–542.
[16] J.E. Sader, Frequency response of cantilever beams immersed in viscous fluids with applications to the atomic force microscope, J. Appl. Phys. 84 (1998) 64–76.
[17] A. Boisen, S. Dohn, S.S. Keller, S. Schmid, M. Tenje, Cantilever-like micromechanical sensors, Rep. Prog. Phys. 74 (2011) 036101.
[18] S. Boskovic, J. Chon, P. Mulvaney, J. Sader, Rheological measurements using microcantilevers, J. Rheol. (1978-Present) 46 (2002) 891–899.
[19] N. McLoughlin, S.L. Lee, G. Hähner, Simultaneous determination of density and viscosity of liquids based on resonance curves of uncalibrated microcantilevers, Appl. Phys. Lett. 89 (2006) 184106.
[20] T.L. Wilson, G.A. Campbell, R. Mutharasan, Viscosity and density values from excitation level response of piezoelectric-excited cantilever sensors, Sensor Actuat. A: Phys. 138 (2007) 44–51.
[21] A. Loui, D. Sirbuly, S. Elhadj, S. McCall, B. Hart, T. Ratto, Detection and discrimination of pure gases and binary mixtures using a dual-modality microcantilever sensor, Sensor Actuat. A: Phys. 159 (2010) 58–63.
[22] I. Dufour, F. Josse, S.M. Heinrich, C. Lucat, C. Ayela, F. Ménil, O. Brand, Unconventional uses of microcantilevers as chemical sensors in gas and liquid media, Sens. Actuators B: Chem. 170 (2012) 115–121.
[23] D. Sparks, R. Smith, J. Patel, N. Najafi, A MEMS-based low pressure, light gas density and binary concentration sensor, Sensor Actuat. A: Phys. 171 (2011) 159–162.
[24] L. Zhao, Y. Hu, R. Hebibul, Y. Xia, L. Huang, Y. Zhao, Z. Jiang, Density measurement sensitivity of micro-cantilevers influenced by shape dimensions and operation modes, Sens. Actuators B: Chem. 245 (2017) 574–582.
[25] R. Cox, J. Zhang, F. Josse, S.M. Heinrich, I. Dufour, L.A. Beardslee, O. Brand, Damping and mass sensitivity of laterally vibrating resonant microcantilevers in viscous liquid media, frequency control and the European frequency and time Forum (FCS), in: 2011 Joint Conference of the IEEE International, IEEE, 2011, pp. 1–6.
[26] L. Beardslee, F. Josse, S.M. Heinrich, I. Dufour, O. Brand, Geometrical considerations for the design of liquid-phase biochemical sensors using a cantilever's fundamental in-plane mode, Sens. Actuators B: Chem. 164 (2012) 7–14.
[27] A. Loui, F. Goericke, T. Ratto, J. Lee, B. Hart, W. King, The effect of piezoresistive microcantilever geometry on cantilever sensitivity during surface stress chemical sensing, Sensor Actuat. A: Phys. 147 (2008) 516–521.
[28] M. Narducci, E. Figueras, M.J. Lopez, I. Gràcia, J. Santander, P. Ivanov, L. Fonseca, C. Cané, Sensitivity improvement of a microcantilever based mass sensor, Microelectron. Eng. 86 (2009) 1187–1189.
[29] H. Hocheng, W.H. Weng, J. Chang, Shape effects of micromechanical cantilever sensor, Measurement 45 (2012) 2081–2088.
[30] I.H. Jafri, H. Busta, S.T. Walsh, Critical point drying and cleaning for MEMS technology, in: Symposium on Micromachining and Microfabrication, International Society for Optics and Photonics, 1999, pp. 51–58.
[31] Y. Özbakır, C. Erkey, Experimental and theoretical investigation of supercritical drying of silica alcogels, J. Supercrit. Fluids 98 (2015) 153–166.
[32] C. García-González, M. Camino-Rey, M. Alnaief, C. Zetzl, I. Smirnova, Supercritical drying of aerogels using CO 2: effect of extraction time on the end material textural properties, J. Supercrit. Fluids 66 (2012) 297–306.
[33] J.S. Griffin, D.H. Mills, M. Cleary, R. Nelson, V.P. Manno, M. Hodes, Continuous extraction rate measurements during supercritical CO 2 drying of silica alcogel, J. Supercrit. Fluids 94 (2014) 38–47.
[34] A. Maali, C. Hurth, R. Boisgard, C. Jai, T. Cohen-Bouhacina, J.-P. Aimé, Hydrodynamics of oscillating atomic force microscopy cantilevers in viscous fluids, J. Appl. Phys. 97 (2005) 074907.
[35] K.D. Tilly, N.R. Foster, S.J. Macnaughton, D.L. Tomasko, Viscosity correlations for binary supercritical fluids, Ind. Eng. Chem. Res. 33 (1994) 681–688.
[36] National Institute of Standards and Technology.

[37] M.D. Fernández-Ramos, L. Cuadros-Rodríguez, E. Arroyo-Guerrero, L.F. Capitán-Vallvey, An IUPAC-based approach to estimate the detection limit in co-extraction-based optical sensors for anions with sigmoidal response calibration curves, Anal. Bioanal. Chem. 401 (2011) 2881.
[38] E. Bakker, P. Bühlmann, E. Pretsch, Carrier-based ion-selective electrodes and bulk optodes. 1. General characteristics, Chem. Rev. 97 (1997) 3083–3132.
[39] D.A. Armbruster, T. Pry, limit of blank, limit of detection and limit of quantitation, Clin. Biochem. Rev. 29 (2008) S49–S52.
[40] L.A. Currie, Detection and quantification limits: origins and historical overview1Adapted from the proceedings of the 1996 joint statistical meetings (American statistical association, 1997). Original title: "Foundations and future of detection and quantification limits". Contribution of the national institute of standards and technology; Not subject to copyright.1, Anal. Chim. Acta 391 (1999) 127–134.
[41] M. Lerchi, E. Bakker, B. Rusterholz, W. Simon, Lead-selective bulk optodes based on neutral ionophores with subnanomolar detection limits, Anal. Chem. 64 (1992) 1534–1540.
[42] L.A. Currie, Limits for qualitative detection and quantitative determination. Application to radiochemistry, Anal. Chem. 40 (1968) 586–593.
[43] G. Gauglitz, Analytical evaluation of sensor measurements, Anal. Bioanal. Chem. (2017).
[44] M.A. O'Connell, B.A. Belanger, P.D. Haaland, Calibration and assay development using the four-parameter logistic model, Chemom. Intell. Lab. Syst. 20 (1993) 97–114.
[45] IUPAC, Pure Appl Chem, 48:127 (1976).
[46] R.M. Lindstrom, Limits for Qualitative Detection and Quantitative Determination, 2009 http://nvl.nist.gov/pub/nistpubs/sp958-lide/164-166.pdf.
[47] E. Voigtman, Limits of Detection in Chemical Analysis, John Wiley & Sons, 2017.
[48] Y. Hayashi, R. Matsuda, K. Ito, W. Nishimura, K. Imai, M. Maeda, Detection limit estimated from slope of calibration curve: an application to competitive ELISA, Anal. Sci. 21 (2005) 167–169.
[49] ISO, Capability of Detection. Part 5: Methodology in the Linear and non-Linear Calibration Cases, International Standardization Organization, Geneva, 2008, pp. 11843–11845, ISO (2008).
[50] IUPAC, Pure Appl Chem, (1976) 45:99–103.

Biographies

Shadi Khan Baloch received his Bachelor's degree in 2008 in Electronics Engineering from Mehran UET Jamshoro in Sindh, Pakistan and worked as Assistant Manager Transmission from 2009 to 2013 in PTCL, the leading telecom company of Pakistan. In 2013, he joined Koç University in Istanbul, Turkey as a PhD student in the Electrical and Electronics Engineering Department. His research interests include using micrcocantilevers in chemical/bio sensing applications.

Alexandr Jonáš received his M.S. degree in Biophysics from Masaryk University in the Czech Republic in 1996 and Ph.D. degree in Physical and Materials Engineering from the Brno University of Technology in the Czech Republic in 2001. He is currently working as a Research Scientist in the Department of Microphotonics at the Institute of Scientific Instruments of the Czech Academy of Sciences in Brno, Czech Republic. His research interests include the development and applications of optical micromanipulation, microscopy, and spectroscopy techniques for characterization of complex systems and environments.

Alper Kiraz is a professor of Physics and Electrical-Electronics Engineering at Koç University. He received his B.S. degree in Electrical-Electronics Engineering from Bilkent University in 1998, M.S. and Ph.D. degrees in Electrical and Computer Engineering from the University of California, Santa Barbara in 2000 and 2002, respectively. He worked as a post-doctoral researcher at the Chemistry Department of the Ludwig-Maximilians University, Munich and as a visiting professor at the Biomedical Engineering Department of the University of Michigan, Ann Arbor. His current research interests include optofluidics, energy photonics, optical manipulation, and biomedical instrumentation.

B. Erdem Alaca Department of Mechanical Engineering, Koc University, Istanbul, 34450, Turkey. B. Erdem Alaca received the B.S. degree in mechanical engineering from Boğaziçi University, Istanbul, Turkey, in 1997, and the M.S. and Ph.D. degrees in mechanical engineering from the University of Illinois at Urbana–Champaign in 1999 and 2003, respectively. He is currently an Associate Professor in the Department of Mechanical Engineering at Koç University, where he manages Mechanical Characterization and Microfabrication facilities. His research interests include mechanical behavior at the small-scale, fabrication technologies and precision instruments based on nano-electromechanical devices. Prof. Alaca is a member of the Turkish National Committee on Theoretical and Applied Mechanics and the Institute of Electrical and Electronics Engineers (IEEE). He was a recipient of the 2009 Distinguished Young Scientist Award from the Turkish Academy of Sciences.

Can Erkey received his B.S. degree in Chemical Engineering in 1984 from Boğaziçi University in Istanbul, Turkey and his Ph.D. degree in 1989 in Chemical Engineering from Texas A&M University in College Station, USA. He served as an assistant professor, associate professor and professor in the Department of Chemical Engineering at the University of Connecticut. He has been a professor in the Chemical and Biological Department at Koc University in Istanbul, Turkey since 2006. He is serving as the Director of the Koc University Tüpraş Energy Center. His research interests are nanostructured materials, energy and supercritical fluids.